

PAPER • OPEN ACCESS

Study on the hydraulic characteristics of side inlet/outlet by physical model test

To cite this article: Bo Kong *et al* 2017 *IOP Conf. Ser.: Earth Environ. Sci.* **61** 012039

View the [article online](#) for updates and enhancements.

You may also like

- [Thermal hydraulic assessment on the full banana model of COOL blanket for CFETR](#)

Kecheng Jiang, Lei Chen, Long Chen et al.

- [Numerical Simulation of Connected Flow in the Inlet and Outlet of the Pumping Storage Power Station](#)

Gaohui Li, Xumin Wu, Minjie Yao et al.

- [Willingness to cooperate in shared natural resource management is linked to group identification through perceived efficacy and group norms](#)

Anna Rabinovich, Lindsay Walker, Deepali Gohil et al.



ECS
The
Electrochemical
Society
Advancing solid state &
electrochemical science & technology

DISCOVER
how sustainability
intersects with
electrochemistry & solid
state science research

Study on the hydraulic characteristics of side inlet/outlet by physical model test

KONG Bo¹, YE Fei², HU Qiu-yue², Zhang Jing³

¹Xi'an University of Technology,

²North China University of Water Conservancy and Electric Power, Zhengzhou 450011, China

³Yellow River Conservancy Commission of the Ministry of Water Resources

corresponding author: Ye Fei, yefei@ncwu.edu.cn, North China University of Water Conservancy and Electric Power, Zhengzhou 450011, China

Abstract. The hydraulic characteristics at the side inlet/outlet of pumped storage plants were studied by physical model test. The gravity similarity rule was adopted and head loss coefficients under pumped and power conditions were given. The flow distribution under both conditions was studied. Scheme of changing the separation pier section area proportion for minimizing velocity uneven coefficient was brought forward and the cause of test error was researched. Vortex evaluation and observation were studied under the pumped condition at normal and dead reservoir water levels.

1. Introduction

The pumped storage plant has a history of more than 100 years. At present, more and more electric power was needed, so the modulation of electric hump and valley became more important than ever before. Due to its electric modulation function, the pumped storage plant can bring huge benefits for economic development. The inlet/outlets of pumped storage plants, according to their pattern, can be classified as side pipe inlet/outlets and vertical pipe inlet/outlets ^[1]. In china, side pipe inlet/outlets are applied more comprehensively. In this paper, the hydraulic characteristics of side inlet/outlets including flow distribution, head loss, vortexes, etc. were researched under pumped and power conditions by physical model test.

Xi-Longchi pumped storage plant lies in Xinzhou, Shanxi province of China, Machine capacity is 1200MW. Downstream reservoir normal water level is 837.0m, dead water level is 798.0m. Design flow head is 624.0m, flow quantity is 54.18 m^3/s under the power condition and 46.76 m^3/s under the pumped condition.

2. Model design and making

2.1. Model design

In order to simulate the prototype exactly, six related variables including Froude number (Fr), Reynold number(Re), Weber number(We), circulation intensity parameter (Nr), relative submergence depth(s/d) and geometrical boundary condition should be taken into account. However, all these variables can not be satisfied at the same time because of mutual exclusion among them^[1]. Considering that the flow in the inlet/outlet is controlled mainly by gravity, the gravity similarity rule was adopted for the physical



model design. The normal model was used for the similarity of flow distribution, submergence depth(s/d) and geometrical boundary condition.

Considering the model material and proving ground, some scales are as follows: model scale, $\lambda_L=39.17$; velocity scale, $\lambda_V=\lambda_L^{0.5}=6.26$; flow scale, $\lambda_Q=\lambda_L^{2.5}=9600.65$; roughness scale, $\lambda_n=\lambda_L^{1/6}=1.84$.

In the prototype, the inhibiting effect on the generation of vortex and circulation by viscosity and surface tension can be ignored because of great values of Re and We . However, in the physical model, the scale effects must be considered^[2]. In order to minimize the scale effects, the Re and We should be above a critical value in mode making. At present, the common critical values are: (1) Suggested by Amphlett^[3], the model Re should be satisfied as $Re = Q/\nu s > 3 \times 10^4$, where Q is the flow quantity, ν is the kinematical viscosity coefficient, s is the submergence depth counted from the orifice center. (2) Suggested by Jain^[4], the model We should be satisfied as $We = \rho V^2 d / \sigma \geq 120$, where V is the orifice average velocity, ρ is the fluid density, d is the orifice height, σ is the surface tension coefficient. The Re and We of the flow in the downstream reservoir inlet/outlet are shown in Tab.1. At different reservoir water levels, both the Re and We were less than the critical values. In order to minimize scale effects, the method of multiplying Q by 2~3 times was adopted for vortex observation in the physical model test^[5]. In this paper, Q was multiplied by 2.2 times and both the Re and We were above the critical values at dead reservoir water level.

Tab.1 The Re and We of flow in the model

Items Conditions	Prototype values				Model values	
	Q (m^3/s)	V (m/s)	d (m)	s (m)	Re (10^4)	We
Design flow quantity	46.76	0.533	6.50	47.68 (normal water level)	0.51	26.67
				7.68 (dead water level)	3.14	
2.2 times Design flow quantity	102.87	1.172	6.50	7.68 (dead water level)	6.91	129.5 2

Annotation: water temperature $15^\circ C$, kinematical viscosity coefficient $\nu = 1.139 \times 10^{-6} m^2 / s$, surface tension coefficient $\sigma = 0.0735 N / m$.

2.2. Model making

The physical model included downstream reservoir, inlet/outlet and part of the tail water tunnel. The inlet/outlets were made of organic glass. The downstream reservoir model was built on a platform(11m×10m) 1.5m height from the ground. Under the power condition, the water provided by the water supply tower flowed into the downstream reservoir via the flowmeters, the tail water tunnel and the inlet/outlets ordinally. Under pumped condition, the water provided by the water supply pool flowed into the downstream reservoir, via the inlet/outlet and the tail water tunnel, finally arrived the stabilized pool. The model plane figure is shown in Fig.1.

Under the pumped condition, Q was measured by the right-angled triangle water measuring weir made according to the Japanese Industry Standard(JIS) and the combined error was $\pm 1.4\%$. Under the power condition, Q was measured by the hole plate flowmeter with a combined error of $\pm 2\%$. The reservoir water level and weir head were measured by water level measuring needle. The velocity distribution at the inlet/outlet was measured by LS-410 direct-reading propeller meter^[6].

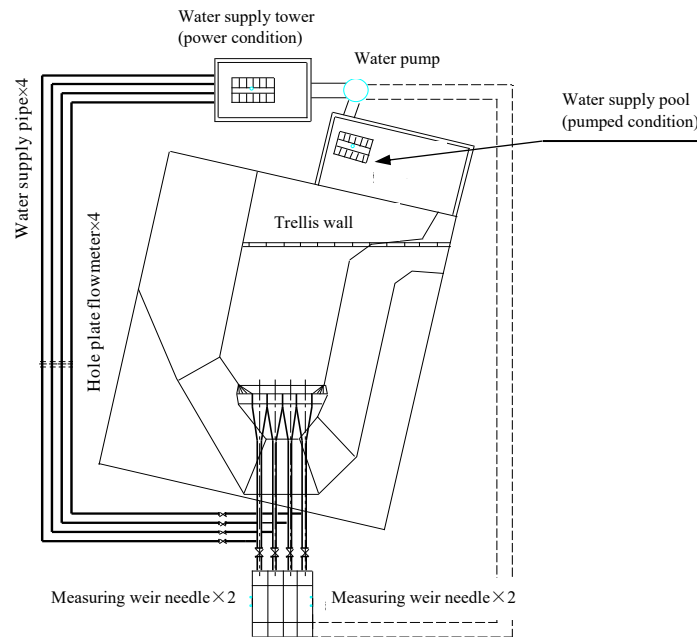


Fig.1 The model ichnography

3. Results and discussion

3.1. Head loss

The head loss of the inlet/outlet, mainly local loss, is very important for hydraulic design and flow condition evaluation. The side inlet/outlet of the downstream reservoir was composed of anti-swirl segment, rectification segment, diffusion segment and transition segment as shown in Fig.2.

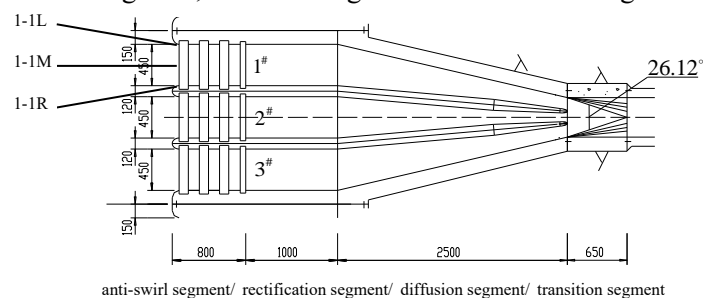


Fig.2 The inlet/outlet ichnography

The head loss was acquired by measuring the reservoir water level (∇_0), the flow quantity and the piezometer tube level (∇_i) at the connective section ($i-i$) of transition segment and tail water tunnel^[7]. According to the Bernoulli Equation, the formulas for head loss under the pumped and power conditions are shown as follows:

$$\text{The pumped condition: } h_{0-i} = \nabla_0 - \nabla_i - \alpha v^2 / 2g \quad (1)$$

$$\text{The power condition: } h_{0-i} = \nabla_i - \nabla_o + \alpha v^2 / 2g \quad (2)$$

$$\text{The head loss coefficient: } \xi = 2gh_f / \alpha v^2 \quad (3)$$

Where h_f is the head loss (f denotes $0-i$ or $i-0$), ξ is the head loss coefficient, v is the average flow velocity of the tail water tunnel, and α is the kinetic energy correction coefficient.

In the prototype, the flow was in square section of flow resistance, so the head loss coefficient was constant and independent of Re and Q. In the model test, the flow was considered to be in square section of flow resistance in the condition that all the head loss coefficients calculated with different Q were basically the same. In this mode test, $Q=31.4\text{m}^3/\text{s} \sim 125.4\text{m}^3/\text{s}$ and $Re=4.8 \times 10^4 \sim 1.9 \times 10^5$ under the pumped condition, and the corresponding values under the power condition were $25.4\text{m}^3/\text{s} \sim 54.2\text{m}^3/\text{s}$ and $3.9 \times 10^4 \sim 8.3 \times 10^4$. As a result, the head loss coefficients under the pumped and power conditions were 0.23 and 0.33, respectively. The head loss coefficient under the power condition was bigger because the diffusion at transverse and vertical direction led to the flow instability.

3.2. Velocity distribution

The flow velocity of each branch orifice (1#, 2# and 3#) was the average value of six measuring points distributed equidistantly along the perpendicular bisector of the section at the trashrack as shown in Fig.2(1-1M). In order to research the change of velocity in transverse direction, the flow velocity of additional perpendicular lines were measured (1-1L, 1-1R).

(1) Pumped condition

In the condition that multi-inlets (inlet 1, 2, 3, 4) worked together, the velocity distribution of each inlet was basically the same as that when it worked alone. The flow velocity of three branch orifices of inlet 1 under different conditions is shown in Fig.3.

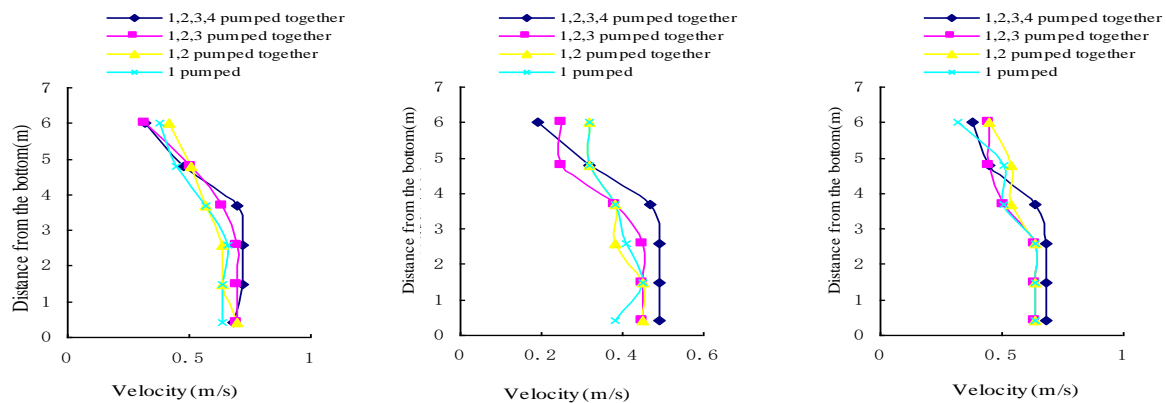


Fig.3 Velocity distribution of inlet1 under different conditions(water level 798.0m, $Q=46.76 \text{ m}^3/\text{s}$)

The velocity distribution at different reservoir water levels is shown in Fig.4. The velocity distribution is basically not influenced by the reservoir water level.

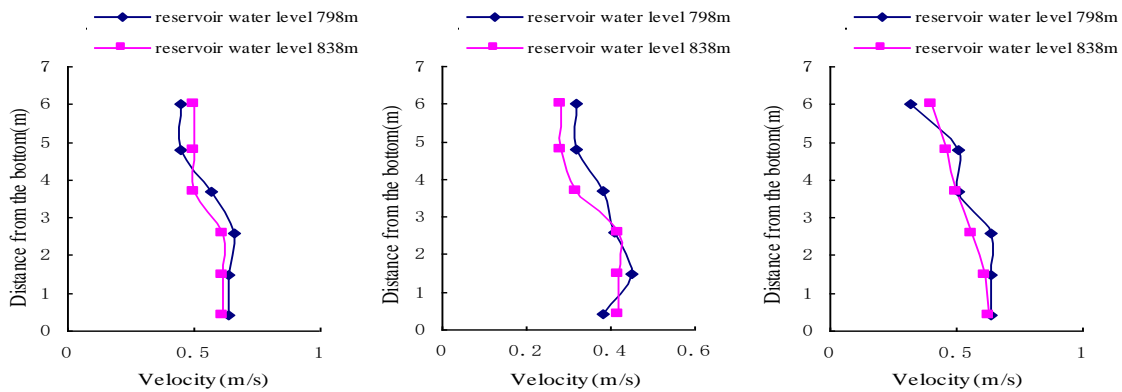


Fig.4 Velocity distribution of inlet1 under different reservoir water levels(Q=46.76 m³/s)

Under different pumped conditions, the average velocity of each branch orifice ranged from 0.42m/s to 0.67m/s, the maximum value was 0.83m/s and the velocity uneven coefficient(the ration of the maximum velocity and average velocity measured at the trashrack) range was 1.21~1.41. For each inlet, the average velocity of the middle orifice (2#) was smaller than that of the two others (1#,3#). The reason is that the section (at the tail of the separation pier) area proportion among the three orifices is 0.35:0.30:0.35. In addition, the press on the flow of the middle orifice by that of the two side orifices at the section also leads to the uneven distribution. This problem can be solved by changing the section area proportion among the three orifices.

Tab.2 The inlet velocity distribution (water level 798.0m, Q=46.76 m³/s)

Inlets	Measured point	1	2	3	4	5	6	Average velocity (m/s)
	Distance from the bottom	0.4 (m)	1.5 (m)	2.6 (m)	3.7 (m)	4.8 (m)	6.0 (m)	
	Branch orifice	velocity (m/s)						
1	1#	0.76	0.76	0.76	0.70	0.48	0.32	0.63
	2#	0.51	0.51	0.51	0.51	0.32	0.19	0.42
	3#	0.70	0.70	0.70	0.64	0.45	0.38	0.59
2	1#	0.76	0.76	0.76	0.64	0.45	0.38	0.63
	2#	0.51	0.51	0.51	0.48	0.35	0.19	0.42
	3#	0.76	0.76	0.76	0.57	0.45	0.32	0.61
3	1#	0.64	0.70	0.70	0.57	0.45	0.41	0.58
	2#	0.51	0.51	0.51	0.45	0.25	0.19	0.40
	3#	0.70	0.70	0.70	0.57	0.45	0.32	0.57
4	1#	0.83	0.76	0.76	0.70	0.45	0.38	0.65
	2#	0.51	0.57	0.57	0.45	0.38	0.22	0.45
	3#	0.83	0.83	0.83	0.7	0.57	0.25	0.67

(2) power condition

In the condition that multi-outlets(outlet1, 2, 3, 4) worked together, the velocity distribution of each outlet was basically the same as that when it worked alone. The flow velocity of three branch orifices of outlet1 under different conditions is shown in Fig.5.

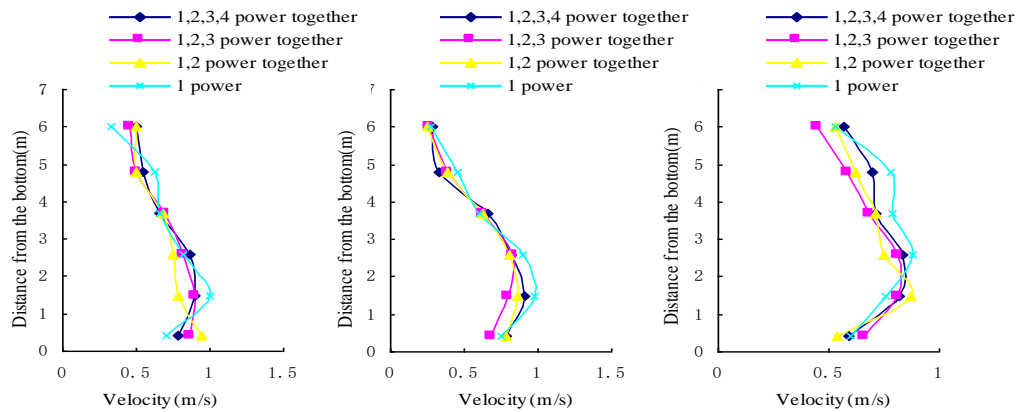


Fig.5 Velocity distribution of outlet1 under different conditions(water level 798.0m, $Q=54.18 \text{ m}^3/\text{s}$)

The velocity distribution of outlet1 at different reservoir water levels is shown in Fig.6. The average flow velocity of each branch orifice at normal water level was less than that at dead water level because of more static water pressure.

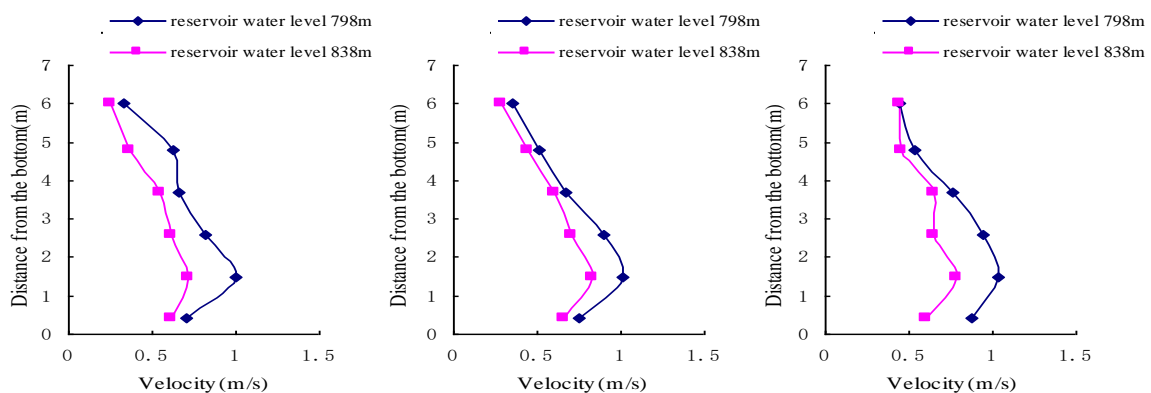


Fig.6 Velocity distribution of outlet1 under different water levels($Q=54.18 \text{ m}^3/\text{s}$)

Under different power conditions, the orifice average velocity ranged from 0.57m/s to 0.73m/s, the maximum value was 1.05m/s and the velocity uneven coefficient range was 1.30~1.58. Compared with the values(1.21~1.41) under the pumped condition, the uneven coefficient was larger because the outflow diffusion at transverse and vertical direction led to flow instability. For each outlet, the average velocity of the middle orifice(2#) was also smaller than that of the two others(1#,3#). This problem can be solved by changing the section area proportion among the three orifices.

The velocity distribution of outlet1 is shown in Fig.7. For its branch orifice 1#, the average velocity acquired from the measurement along 2-1L, 2-1M and 2-1R were 0.73 m/s, 0.81 m/s and 0.64 m/s, it indicated that the main flow deflected to the left side(facing the upstream direction). For the branch orifice 3#, the corresponding values were 0.62 m/s, 0.85 m/s and 0.78 m/s, therefore, the main flow deflected to the right side. However, the average velocity of branch orifice 2# measured along different lines were basically the same and no deflection was found. Therefore, in order to minimize test errors, the velocity of three perpendicular lines should be measured for calculating the average velocity of branch orifice 1# and 3#.

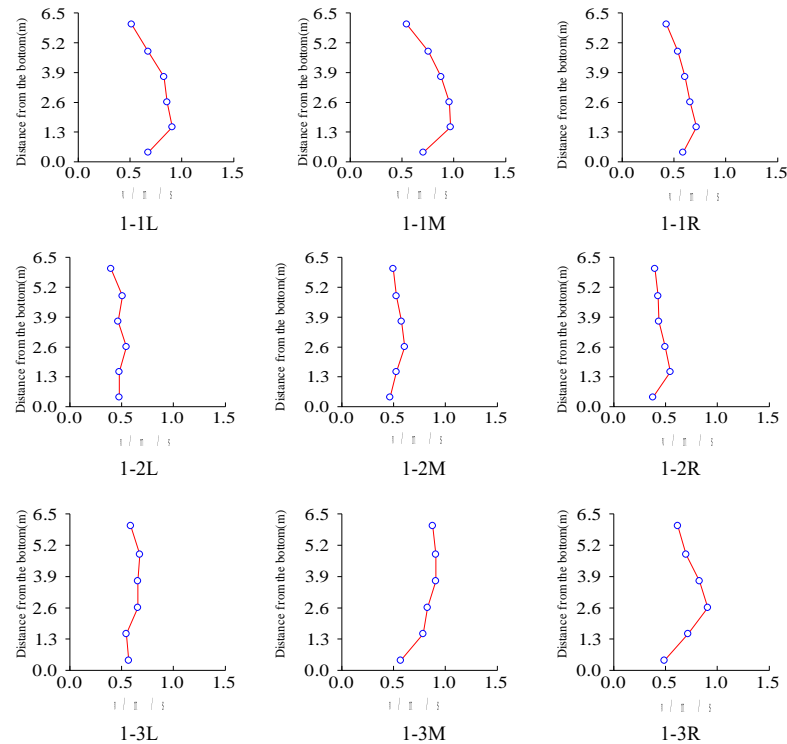


Fig.7 Velocity distribution of outlet1(water level 798.0m, $Q= 54.18 \text{ m}^3/\text{s}$)

3.3. Vortexes

According to the observation data of 29 prototype inlets, Gordon *et al.* made the conclusion^[8] that the generation of vortexes related to the velocity, inlet dimension and submergence depth. The critical submergence depth without vortexes can be described as:

$$S_c = CVd^{1/2} \quad (4)$$

where S_c is the critical submergence depth calculated from the top of the inlet, d is the inlet height, V is the flow velocity of tail water tunnel, C is the coefficient, ($C = 0.55$ for symmetry inflow, and $C = 0.73$ for dissymmetry inflow). According to the prototype data ($V = 0.53 \text{ m/s}$, $d = 6.5 \text{ m}$), the S_c calculated was 0.94 m , lower than the submergence depth (4.334 m) at dead water level.

According to the data of 13 prototype inlets, Pennino *et al.* draw the conclusion^[9] that the inlet Fr without vortexes should be expressed as:

$$Fr = V / \sqrt{gs} < 0.23 \quad (5)$$

where s is the submergence depth calculated from the centre of the inlet, V is the flow velocity, g is the acceleration of gravity. There are almost no vortexes generation if $Fr = 0.06 < 0.23$ and $s/d > 0.5$, where d is the inlet height. Tab.3 shows the vortex evaluation of the inlet according to the prototype data.

Tab.3 The vortex evaluation of the inlet

Flow quantity $Q(\text{m}^3/\text{s})$	Flow velocity $V(\text{m}/\text{s})$	Orifice height $d(\text{m})$	Reservoir water level $\nabla(\text{m})$	Submergence depth $s(\text{m})$	F_r	s/d	Harmful vortexes (Y/N)
46.76	0.53	6.50	Normal water level	47.584	$0.03 <$	$7.3 > 0.5$	N
			838.0	7.584	0.23	$1.2 > 0.5$	N
			Dead water level		$0.06 <$		
			798.0		0.23		

In the model test, in order to minimize scale effects, Q was multiplied by 2.2 times for vortex observation. When the water level changed from the normal water level to the dead water level, no harmful vortexes (air suction vortexes or other adsorption vortexes) generated.

4. Conclusions

In this paper, the flow characteristics of side inlet/outlets were studied by physical model test. The head loss coefficients under the pumped and power conditions were 0.23 and 0.33, respectively. The value under the power condition was larger because the flow diffusion at transverse and vertical direction led to the flow instability.

In the condition that multi-inlet/outlets worked together, the velocity distribution of each inlet/outlet was basically the same as that when it worked alone. The flow distribution was basically not influenced by the reservoir water level under the pump condition, however, under the power condition, The average flow velocity of each branch orifice at normal water level was less than that at dead water level because of more static water pressure. For each inlet/outlet, the average velocity of the middle orifice was smaller than that of the two others, and this problem can be solved by changing the section area proportion among the three orifices. Under the power condition, the main flow of the left (or right) branch orifice deflected from the center to the left (or right) side, in order to minimize test errors, the velocity of three perpendicular lines should be measured for calculating the average velocity of the two side branch orifices.

Under the pumped condition, when the water level changed from the normal level to the dead level, no harmful vortexes generated.

References

- [1] Lu You-mei, Pan Jia-zheng. the Pumped Storage Plant [M]. Bei Jing: Water conservancy and Electric power publisher, 1992, Modeling Hydraulic Structures
- [2] Hecker, G.E, S cale effects in vortexes simultion, Symposium on Scale Effects in, Yangtse Rive water and electricity science academe, 1985.10, 219-237.
- [3] Amphlett, M.B, et al. Similarity of Free-Vortex at Horizontal Intake[J]. Journal of Hydraulic Research, 1978, 16(2): 95-105
- [4] Jain, A.K, et al. Vortex Formation at Vertical Pipe Intake[J]. Journal of the Hydraulics Division, 1978, 104(10):1429-1445
- [5] Hecker, G.E. Model-prototype comparison of free surface vortices[J]. Journal of the Hydraulics Division, 1981, 107(10):1243-1259
- [6] Tianjin University, Beijing Water conservancy and Electric power Comporation. Report of the up reservoir inlet/outlet of Xilongchi power station[R]. 2002
- [7] H.K.Versteeg, W. Malalasekera. An introduction to computational fluid dynamics[M]. New York: Longman Scientific & Technical, 1995
- [8] Gordon J L, Wortexes at vertical intakes[J]. Water Power, 1970, (4): 137-138
- [9] M.Syamlal, T.J.Brien. Computer Simulation of Bubbles in a Fluidized Bed[J]. AICHE Symp Series, 1989, 85(1): 22-31